FABRICATION AND CHARACTERIZATION OF HIGH CURRENT-DENSITY, SUBMICRON, NbN/MgO/NbN TUNNEL JUNCTIONS

J. A. Stern

H. G. LeDuc

*A. J. Judas**

Center for Space Microelectronics Technology
Jet Propulsion Laboratory
California Institute of Technology
Pasadena, California 91109
* Present Address: Stanford University
Palo Alto, California

Abstract

At near-millimeter wavelengths, heterodyne receivers based on SIS tunnel junctions are the most sensitive available. However, in order to scale these results to submillimeter wavelengths, certain device properties should be scaled. The tunnel-junction's current density should be increased to reduce the RC product. The device's area should be reduced to efficiently couple power from the antenna to the mixer. Finally, the superconductor used should have a large energy gap to minimize RF losses. Most SIS mixers use Nb or Pb-alloy tunnel junctions; the gap frequency for these materials is approximately 725 GHz. Above the gap frequency, these materials exhibit losses similar to those in a normal metal. The gap frequency in NbN films is as-large-as 1440 GHz. Therefore, we have developed a process to fabricate small area (down to 0.13 μ^2), high current density, NbN/MgO/NbN tunnel junctions.

In this paper, we describe a process used to fabricate submicron NbN junctions. Low-leakage current-voltage (I-V) characteristics are achieved for current densities up to 40 kA/cm^2. However, the quality of the I-V characteristics degrades significantly for higher current densities. Junction areas are patterned by lifting off a Cr stencil defined by electron beam lithography. This image is transferred to a polyimide stencil using reactive ion etching (RIE). The junctions are then etched and isolated using a self-aligned liftoff technique. The limitations of this technique and the quality of the resulting I-V characteristics will be discussed.

There are several device and materials parameters which must be known to properly design mixer circuits. The optimal imbedding impedance for the mixer is determined by the capacitance and I-V characteristic of the tunnel junction. If microstrip line circuits are used to achieve this impedance, the magnetic penetration depth of the NbN must be known to calculate the microstrip line impedance and propagation velocity. We have measured the junction capacitance versus current density and microstrip line inductance using superconducting quantum interference devices (SQUIDs). The propagation velocity was measured using long open-ended microstrip-lines connected to Josephson tunnel junctions. The magnetic penetration depth can be calculated from either the microstrip line inductance or the propagation velocity. The implications of these measurements will be discussed.

Introduction

There is a growing need for sensitive submillimeter (smm) wavelength detectors for both ground based and space based applications. Heterodyne receivers based on superconductor-insulator-superconductor (SIS) tunnel junctions are the most sensitive at millimeter and near-millimeter

wavelengths [1][2]. At wavelengths longer than 3 mm, the noise in these detectors has approached the quantum limit [3]. If these mixers designs could be redesigned for shorter wavelength operation, they would fill the need for smm wavelength mixers. For good performance to be achieved at smm wavelengths, a number of SIS tunnel junction properties must be adjusted. We have fabricated and characterized tunnel junctions which are suitable for smm use.

The junction capacitance is the property which has the largest impact on smm wave mixers. An SIS tunnel junction can be modeled as a nonlinear tunneling element in parallel with a shunt capacitance. The product of the shunt capacitance (C) and the RF resistance of the junction (approximately the normal state resistance, R_n) is one limit on the high frequency response of a tunnel junction, because the capacitance tends to shunt RF currents away from the nonlinear tunneling element. To reduce the R_nC time constant, the tunnel junction barrier is made thinner; this increases the junction capacitance

$$C=\epsilon_0\epsilon_r A/d,$$

where ϵ_0 is the dielectric constant of free space, ϵ_r is the relative dielectric constant of the barrier, A is the junction area and d is the barrier thickness, but it decreases the resistance more rapidly

$$R_n=\frac{h^2 d\cdot\exp\{4\pi d\sqrt{2m\phi}/h\}}{e^2 A\sqrt{2m\phi}}$$

where h is Plank's constant, m is the mass of the quasi-particle, ϕ is the barrier height and e the charge of the quasiparticle. Because the barrier cannot be made thinner than one monolayer, the R_nC product is ultimately limited by the barrier material properties (ϵ_r, ϕ and the lattice

constant). The R_nC product is independent of junction area, but the junction resistance must be roughly 100 Ω for it to couple efficiently to the antenna. Therefore, as the barrier is made thinner, the tunnel junction's area must also be reduced. At smm wavelengths, junctions with submicron areas are needed. Since the barrier thickness is difficult to measure, R_nA products can be used as an area-independent measure of junction relaxation time. The product of the critical current density (J_c) and R_nA is proportional to the energy gap, so the current density is also frequently used as a measure of the relaxation time.

The embedding circuit of a mixer can be designed to resonate out the junction capacitance over a frequency band. In waveguide mixer mounts, this can be accomplished using a back short and E-plane tuner; however, at high frequencies these tuners do not work as well as at lower frequencies. Additionally, quasi-optical mixers do not have these tuning elements. Monolithic embedding circuits can also be fabricated to resonate out the junction capacitance [4][5][6]. Many of these circuits use superconducting microstrip lines. To accurately design these circuits, the propagation velocity and impedance of the microstrip line must be known. Both of these parameters depend critically on the magnetic penetration depth of the superconductor [7].

The energy gap of the superconductor (2Δ) limits the use of SIS mixers at smm wavelengths. Above the gap frequency ($2\Delta/h$), the superconductor has losses similar to those in a normal metal; therefore, any embedding circuits will have losses[8]. Embedding circuits could be made of a larger gap superconductor or a low-loss normal metal (such as gold or copper). In this case, the SIS mixer will perform well up to twice the gap frequency. Most mixers currently use

niobium based tunnel junctions. The gap frequency of niobium is 725 GHz. Above this frequency, other superconductors will probably be needed.

Based on the small gap in niobium, we have developed a process for fabricating junctions with NbN electrodes, which has a much larger gap frequency (up to 1440 GHz). The goal was to fabricate high current-density, submicron tunnel junctions with large energy gaps. The limitations of our process on both current density and junction area are discussed below. Additionally, we have measured several device properties necessary to design mixer circuits (NbN magnetic penetration depth, junction uniformity, yield and specific capacitance.)

Junction Fabrication

The tunnel junctions are fabricated by depositing the NbN/MgO/NbN trilayer over the entire substrate [9][10]. The NbN films are deposited by reactive DC-magnetron sputtering from a niobium target using a 5 cm diameter US inc. sputter gun in an argon and nitrogen atmosphere. The gas flow rates are 150 and 15 sccm respectively and the total pressure with the plasma off is 14.4 mTorr. The gun is typically biased at -232 Volts and 600 mAmps. The substrate is not heated and is approximately 6 cm from the sputter gun. Deposition rates are 45 nm/min. The thickness of the base and counter electrode are 315, 135 nm respectively. The superconducting transition temperature of the films is usually between 14.5 and 15.0 K.

The barrier layer is formed by depositing MgO and performing a pinhole cure in an oxygen plasma. MgO is deposited by RF sputtering from a US inc. 5 cm diameter source in a pure argon atmosphere. The Ar pressure is 10.0 mTorr and the power is 50 Watts. To promote

uniform growth of the barrier, deposition occurs intermittently as the substrate is rotated past the source in a circular orbit. After the barrier deposition, the sample is exposed to an oxygen-plasma glow discharge for 1 minute at 100 mTorr. The plasma is maintained with a high purity aluminum ring below the substrate; the ring is biased at -400 Volts and 2.0 mA. Barrier deposition times vary between 5.5 and 6.7 min. for current densities between 40 and 10 kA/cm^2.

The trilayer is completed by covering the entire NbN/MgO/NbN structure with 30 nm of gold. The gold prevents the top surface of the junction from oxidizing in air. In some cases, there is a thin (40 nm) layer of Nb between the counter electrode and the gold. The purpose of the Nb interlayer will be discussed below.

Tunnel junctions are fabricated using a submicron, self-aligned lift-off technique. This process is shown in figure 1. The trilayer is patterned using RIE and a photoresist stencil. The etcher used is a Semi Group System 1000, and the electrode area is 730 cm^2. The gold and MgO layers are etched using a straight argon sputter etch. The NbN layers are etched in a CF_4-O_2 mixture. The conditions for this and other reactive ion etches are given in table 1. After the etch, the photoresist is stripped in organic solvents.

The submicron tunnel junction stencil is formed in a polyimide layer [11]. The etched trilayer is coated in Ciba Geigy Probimide 286 and thinner 2:1 at 4000 rpm resulting in a 310 nm polyimide layer. The polyimide is cured at 150° C on a hot plate for 15 minutes and flood exposed with 315 nm radiation. A KTI Chemicals Inc. 950K 2% PMMA layer is spun on top of the polyimide at 4000 rpm and baked at 150° C. A thin aluminum layer is evaporated on top

of the PMMA to prevent charging during the exposure. The sample is exposed in a JEOL model JBX5 electron beam lithography system and subsequently developed to reveal square holes in the PMMA. A thin (35 nm) chromium layer is thermally evaporated and lifted off to define the junction area. Next an AZ 5214-E stencil is patterned using image reversal [12] to reveal an open area around the chromium dot. This stencil acts to protect the majority of the trilayer from the junction etch. The polyimide layer is etched using an oxygen plasma. During the etch, a polyimide (Kapton) sheet is about 3 cm above the sample to protect against particles falling on the sample during the etch. The oxygen etch is very anisotropic and an over etch is normally used to insure that the trilayer surface is completely clean.

The junction etch consists of an Ar sputter-etch of the gold and one of several NbN etches [13]. For micron size junctions, the CF_4-O_2 mixture can be used, however this etch is isotropic and it will undercut NbN mesa. A straight CF_4 etch can be used for submicron junctions. This etch is largely anisotropic, because a fluorinated carbon layer forms on the sidewall of the junction as it etches; however, there is about 50 nm of undercut. A mixture of CCl_2F_2-CF_4-O_2 produces an anisotropic etch, however it reacts at the Au-NbN interface and produces a superconductor-normal metal-superconductor type I-V characteristic in series with the SIS I-V characteristic. This series weak link can be avoided by inserting a niobium layer between the gold and NbN layers and by rinsing the sample in water after the etch. The niobium buffer removes the series weak link which seams to occur at the NbN-Au interface Regardless of the etch used, a monitor sample is used to detect the endpoint of the junction etch. After the junction etch, a 1 minute argon sputter etch is done to improve the adhesion of the dielectric isolation layer.

Table 1. Summary of Reactive Ion Etch Conditions

Material	Etch Gases	Flow Rates (sccm)	Pressure (mTorr)	Power (Watts)	Etch Rate (nm/min)
Polyimide	O_2	20	30	130	100
Gold	Ar	20	30	118	15
NbN	CF_4,O_2	20,2	30	118	65
NbN	CF_4	20	30	118	52
NbN	CCl_2F_2, CF_4,O_2	23,7,2	30	118	58

The junction is electrically isolated by thermally evaporating 150 nm of Silicon monoxide on the sample. The wafer is rotated at a 5 to 15° angle during the evaporation to improve SiO coverage. The photoresist protection layer is then lifted off in acetone, followed by the polyimide in dichloromethane. The polyimide liftoff is done in an ultrasonic cleaner followed by a mechanical scrub with a q-tip to remove the SiO flags that form on the side-walls of the polyimide pillar. The liftoff yield, even for the smallest junctions, is excellent. Following the polyimide liftoff, an oxygen etch is done to remove any polyimide residue which will lead to a contact resistance.

The NbN wiring layer is deposited on top of the electrically isolated junction. To avoid breaks at step edges, the wiring is typically 600 nm thick. The wiring is patterned and etched like the trilayer, although if small features are desired, one of the anisotropic etches is used.

Results

The quality of tunnel junction I-V characteristics depends strongly on the critical current density. As the current density increases, the ratio of the subgap resistance (measured at 3 mV) to the normal state resistance decreases. Figure 2 shows a plot of this ratio as a function of critical current density. Above 50 kA/cm^2, the ratio R_{sg}/R_n is reduced to two; however, for current densities up to 40 kA/cm^2 the I-V characteristics are still reasonable. An example of a 0.42x0.42 μ^2, 35 kA/cm^2 junction is shown in figure 3; this junction was fabricated for 626 GHz mixer tests.

A second form of I-V degradation occurs at high current densities. For a fixed area junction, the gap voltage decreases as the current density increases. This is caused by a non-thermal distribution of quasi-particles near the barrier. As the tunneling current increases, the number of quasi-particles injected into the superconducting electrode increases; this represents a local heating of the quasiparticle bath and leads to a reduction in the gap voltage. The quasi-particle heating can be minimized by reducing the junction area. Table 2 shows the gap for different area junction on the same wafer; the current density is 28 kA/cm^2.

Table 2. Energy Gap as a Function of Junction Size

size (microns)	Energy Gap (meV)
1.0	4.15
0.7	4.3
0.5	4.4
0.36	4.45

Junction uniformity and yield was measured by fabricating series arrays of 100 tunnel junctions. Typical I-V characteristics for arrays of 0.49, 0.25 and .13 μ^2 junctions are shown in figure 4. For these size junctions, the standard deviation of the critical currents is typically $\pm$5.4, 6.6 and 7.7% respectively. For comparison, the standard deviation for optically defined, 4 μ^2 junctions is 3.9%. Typical minimum-to-maximum uniformity is $\pm$17% for 0.25 μ^2 junctions. When the fabrication process was successful, junction yields were better than 99 %. The uniformity and yield for this process were high enough that a monolithic array of mixers could be fabricated.

SQUIDs have been fabricated to measure the magnetic penetration depth of NbN films and the specific capacitance of NbN/MgO/NbN junctions. The design of the SQUIDs is based on that of Magerlein [14] and is described in detail elsewhere [15]. Briefly, the SQUID design is a microstrip line over a ground plane with two tunnel junctions connecting the microstrip to the ground plane. The inductance of the microstrip line, and therefore the magnetic penetration depth, can be determined by observing the critical current of the two parallel-junctions versus control current passing along the microstrip line. The loop of the SQUID and the junction capacitance form an LC tank circuit. The Josephson oscillations will interact with this tank circuit to form a current step at a voltage proportional to this resonant frequency. The junction capacitance can be determined from the resonance voltage and the critical-current modulation curve.

The magnetic penetration depth can also be determined using an open-ended microstrip-line connected to a Josephson junction. The microstrip line has an impedance which is periodic with frequency. The Josephson oscillations interact with the microstrip line circuit to yield a series

of resonances whenever the microstrip line reflects an inductance that cancels out the junction capacitance. An example of these resonances is shown in figure 5. The propagation velocity of the microstrip line can be calculated to be

$$V_p = e \cdot \delta V / h \cdot 2L,$$

where δV is the spacing or the resonances and L is the length of the microstrip line stub. The penetration depth can be calculated from the propagation velocity. These microstrip line stubs are a good method of verifying the SQUID results and directly measuring the microstrip line propagation velocity.

The specific capacitance of our junctions as a function of J_c is shown in figure 6 for critical current densities ranging from 500 to 50,000 A/cm^2. Much of this data has been published previously[14]; however, we have extended the data to include the highest current densities shown here (10 to 40 kA/cm^2). Also shown in figure 6 is the R_nC frequency as a function of current density. At 40 kA/cm^2, the roll off frequency is only 140 GHz; therefore, at smm wavelengths, the capacitance must be tuned out to achieve optimal performance.

The magnetic penetration depth of our NbN films has also been measured using SQUIDs. The penetration depth varies significantly with film quality and is typically between 270 and 380 nm. The propagation velocity of microstrip lines with 150 nm SiO dielectric layers is typically 0.16 to 0.18 times the speed of light in a vacuum. The penetration depth calculated from these numbers is 300 to 365 nm, which agrees well with the SQUID results. Because the penetration depth depends critically on film quality, SQUID and microstrip line circuits are usually added to mixer mask-designs, so the penetration depth can be measured for each set of tunnel junctions

that are fabricated. These circuits are small (2.5 mm × 2.5 mm) and 12 test dies take up roughly one sixth of a 25 mm diameter quartz wafer.

Conclusions

We have developed a process for fabricating high critical current, submicron NbN/MgO/NbN tunnel junctions. The yield and uniformity of this process is good and should be sufficient for most mixer needs. However, the R_nC frequency can only be made 140 GHz without seriously degrading the I-V quality. Submillimeter wave mixers will either require high Q circuits to resonate out the junction capacitance or a new barrier material with a lower dielectric constant or barrier height. Although NbN films should have low RF losses even at smm wavelengths, the actual losses need to be measured in order to evaluate potential high Q tuning circuits. In addition, the effects, if any, of quasi-particle heating on mixer performance need to be investigated.

Work Supported by NASA and SDI/IST

References

[1] C. K. Walker, M. Chen, P. L. Shafer, H. G. LeDuc, J. E. Carlstrom and T. G. Phillips, "A 492 GHz SIS Waveguide Receiver for Submillimeter Astronomy," *Int. J. of IR and Millimeter Waves,* Submitted 1992.

[2] T. H. Buttgenbach, H. G. LeDuc, P. D. Maker and T. G. Phillips, "A Fixed Tuned Broadband Matching Structure for Submillimeter SIS Receivers," *IEEE Trans. Appl. Superconductivity,* Submitted Feb. 1992.

[3] C. A. Mears, Qing Hu, P. L. Richards, A. H. Worsham, D. E. Prober and A. V. Räisänen, "Quantum Limited Quasiparticle Mixers at 100 GHz," *IEEE Trans. on Magn.,* vol. 27, no. 2, 1991.

[4] L. R. D'Addario, "An SIS Mixer for 90-120 GHz with Gain and Wide Bandwidth," *Int. J. of IR and Millimeter Waves,* vol. 5, no. 11, 1419-1442, 1984.

[5] A. V. Räisänen, W. R. McGrath, P. L. Richards and F. L. Lloyd, "Broad-Band Match to a Millimeter-Wave SIS Quasi-Particle Mixer," *IEEE Trans. on Microwave Theory and Technique,* vol. 4, no. 12, December 1985.

[6] S. K. Pan, A. R. Kerr, M. J. Feldman, A. W. Kleinsasser, J. Stasiak, R. L. Sandstrom and W. J. Gallagher, "An 85-116 GHz SIS Receiver Using Inductively Shunted Edge-Junctions ," *IEEE Trans. on Microwave Theory and Technique,* vol. 37, no. 3, 580-592, March 1989.

[7] W. H. Chan, "The Inductance of a Superconducting Strip Transmission Line," *J. Appl. Phys.*, vol.50, no. 12, Dec. 1979.

[8] R. L. Kautz, "Picosecond Pulses on Superconducting Striplines," *J. Appl. Phys.*, vol. 49, 308-314, 1978.

[9] H. G. LeDuc, J. A. Stern, S. Thakoor and S. Khanna, "All Refractory NbN/MgO/NbN Tunnel Junctions," *IEEE Trans. Magn.* vol. 23, March 1987.

[10] J. A. Stern, B. D. Hunt, H. G. LeDuc, A. Judas, W. R. McGrath, S. R. Cypher and S. K. Khanna, "NbN/MgO/NbN SIS Tunnel Junctions for Submm Wave Mixers," *IEEE Trans. Magn.*, vol 25, 1989.

[11] A. W. Lichtenberger, D. M. Lea, C. Li, F. Lloyd, M. J. Feldman and R. J. Mattauch, "Fabrication of Micron Size Nb/Al-Al_2O_3/Nb Junctions with a Trilevel Resist Liftoff Process," *IEEE Trans on Magnetics,* vol. 27, no. 2, March 1991.

[12] M. Spak, D. Mammato, S. Jain and D. Durham, "Mechanism and Lithographic Evaluation of Image Reversal in AZ 5214 Photoresist," As Presented at: *Seventh International Technical Conference on Photopolymers, Ellenville, New York,* Reprints Available from American Hoechst Corporation, AZ Photoresist Products.

[13] H. G. LeDuc, A. Judas, S. R. Cypher, B. Bumble, B. D. Hunt and J. A. Stern, "Submicron Area NbN/MgO/NbN Tunnel Junctions For SIS Mixer Applications," *IEEE Trans. on Magnetics,* vol. 27, no. 2, March 1991.

[14] J. H. Magerlein, "Specific Capacitance of Josephson Tunnel Junctions," *IEEE Trans. Magn.*, vol. 17, no. 2, 286-289, 1981.

[15] J. A. Stern and H. G. LeDuc, "Characterization of NbN Films and Tunnel Junctions," *IEEE Trans. Magn.*, vol 27, no. 2, March 1991.

Figure Captions

Figure 1 *Submicron, self-aligned liftoff process.*

Figure 2 *Subgap resistance divided by the normal state resistance as a function of critical-current density*

Figure 3 *I-V characteristic of a .42x.42 μ^2, 35 kA/cm^2, tunnel junction. The current scale is 20 μA/div. and the voltage scale 1 mV/div.*

Figure 4 *I-V characteristics for series arrays of 100 tunnel junctions. The voltage scale is 50 mV/div. The area of the junctions is 0.13, 0.25, 0.49 μ^2, and the current scale is 10 20 and 50 μA/div for figures a, b and c respectively.*

Figure 5 *I-V characteristic of a 1 μ^2 tunnel junction connected to a 6 μ by 750 μ open-ended microstrip-line stub. The current scale is 5 μA/div, and the voltage scale is 100 μV/div. The resonance spacing is 65 μV leading to a propagation velocity of 0.16 times the speed of light.*

Figure 6 *Junction specific capacitance (a) and R_nC roll-off frequency ($1/2\pi R_nC$) (b) as a function of critical-current density.*

Figure 1.

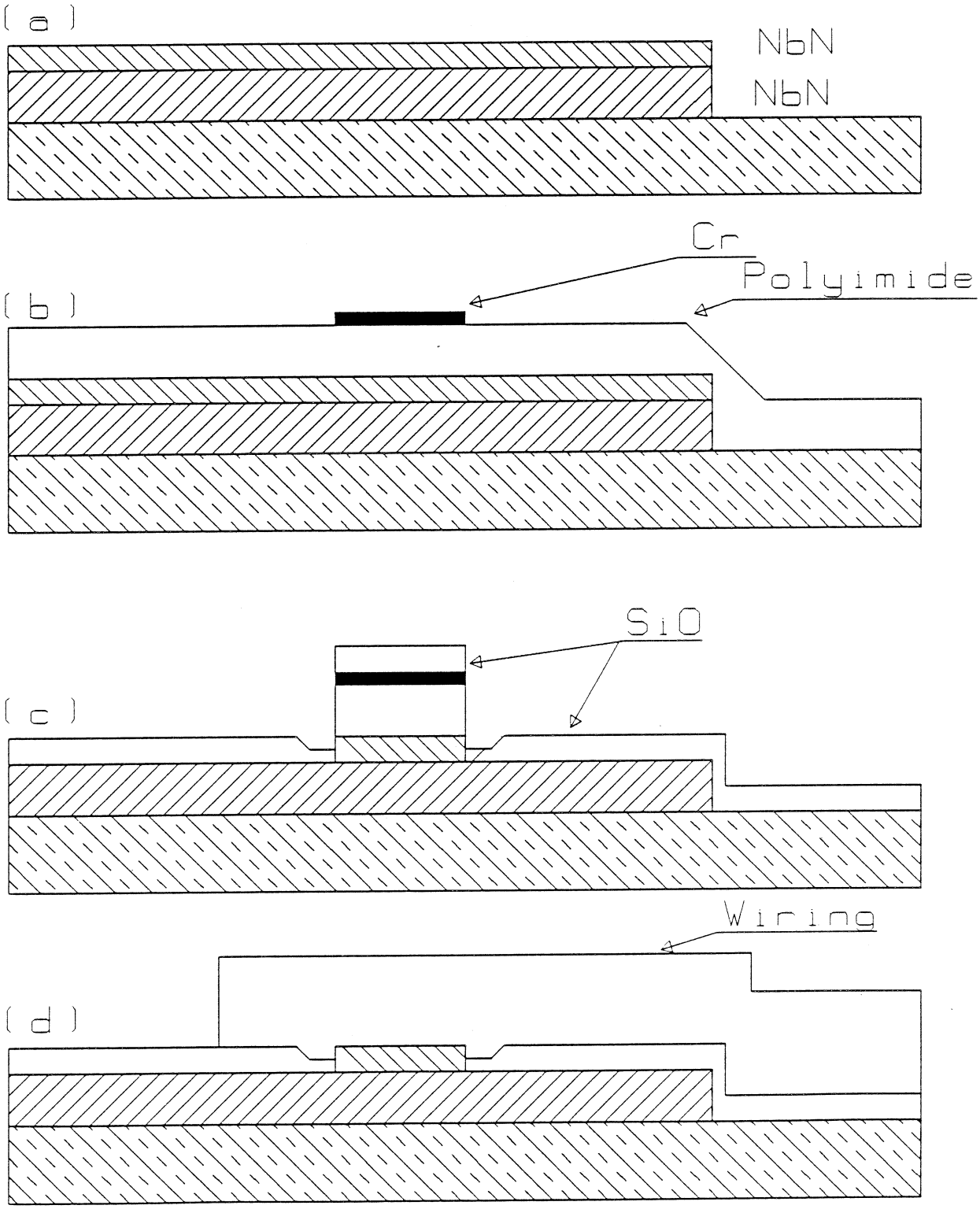

Figure 2.

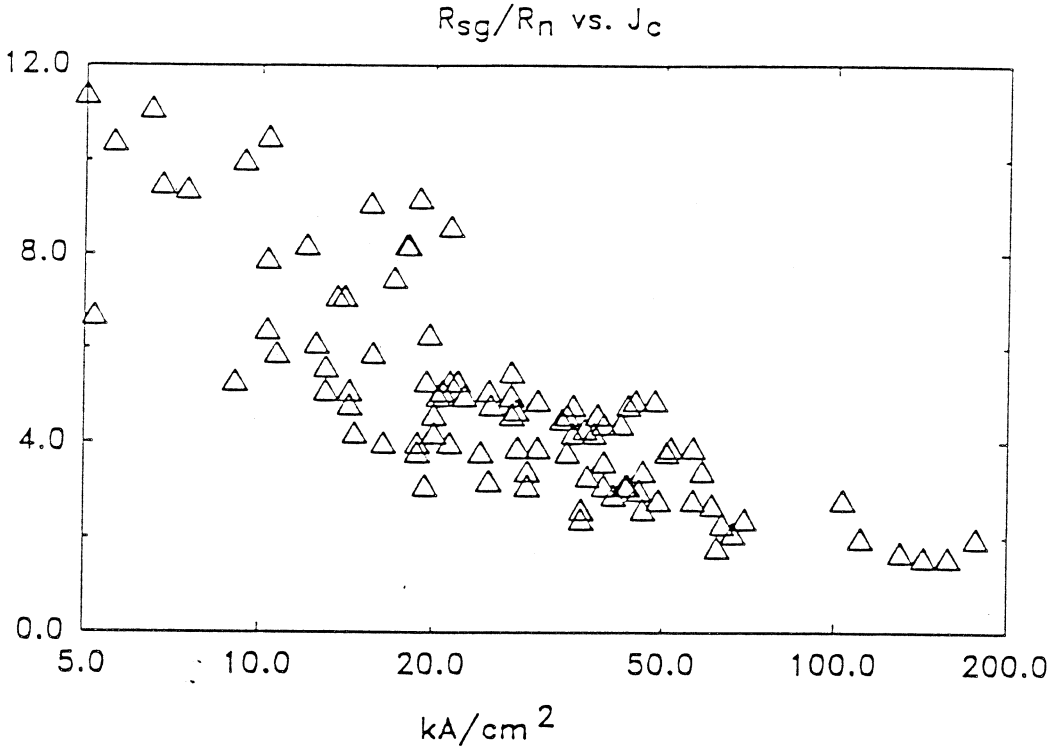

Figure 3.

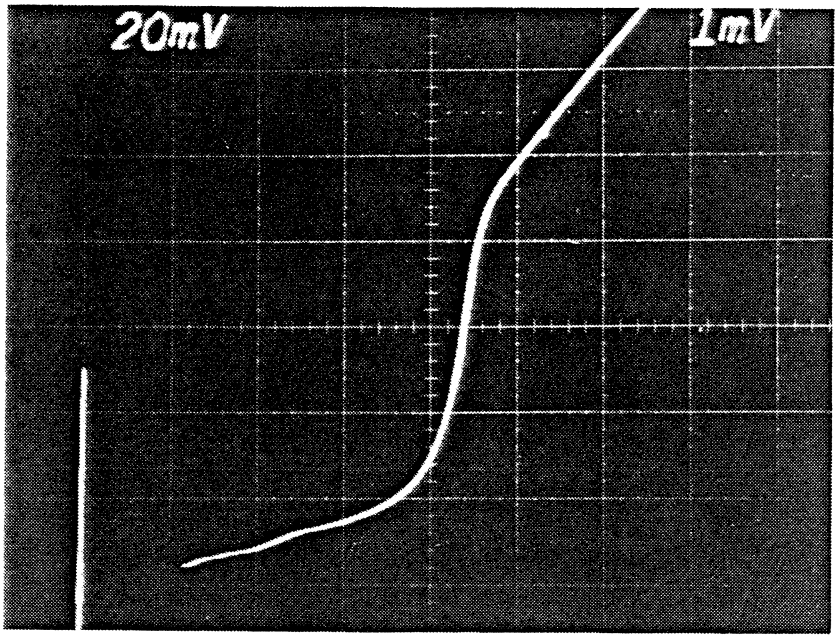

Figure 4.

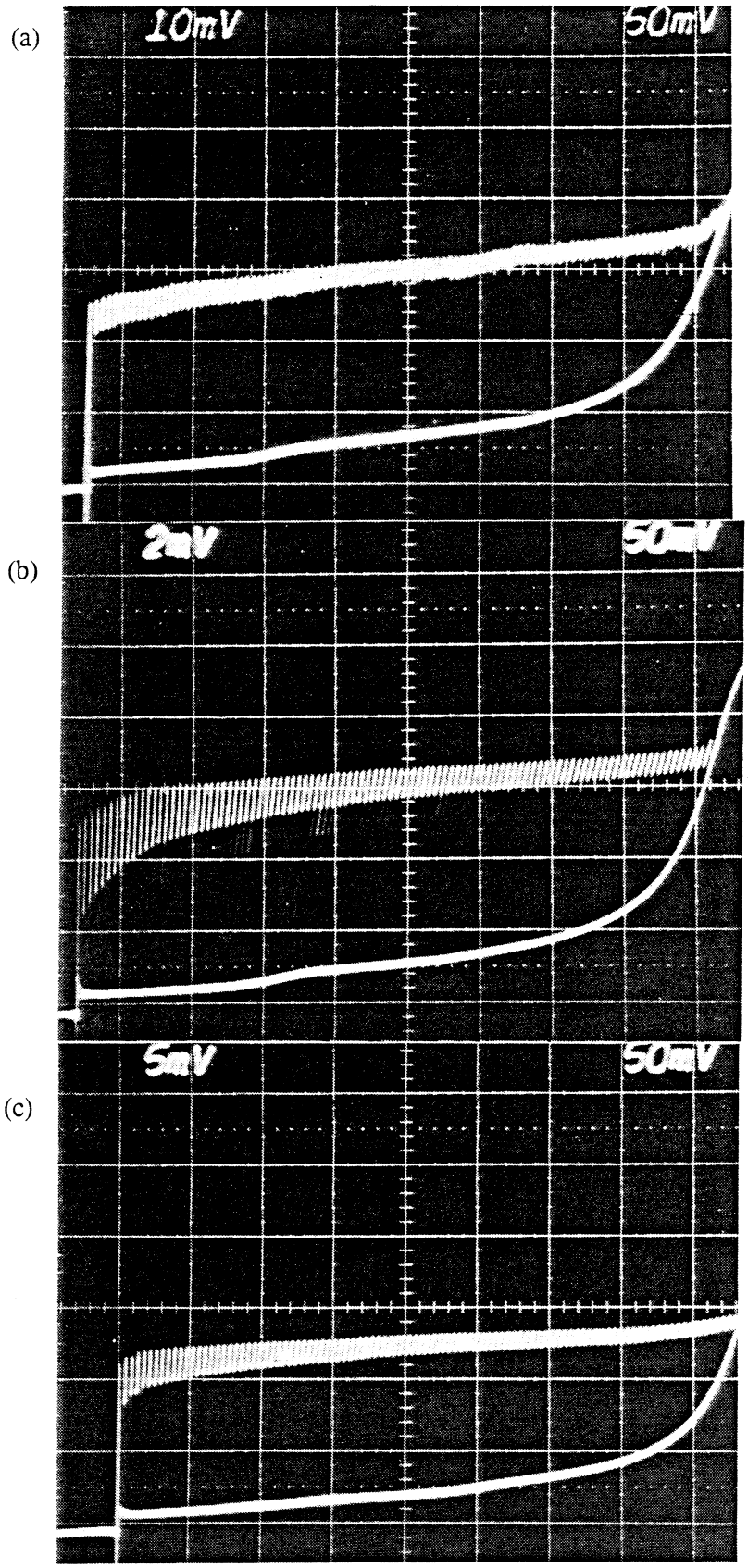

Figure 5.

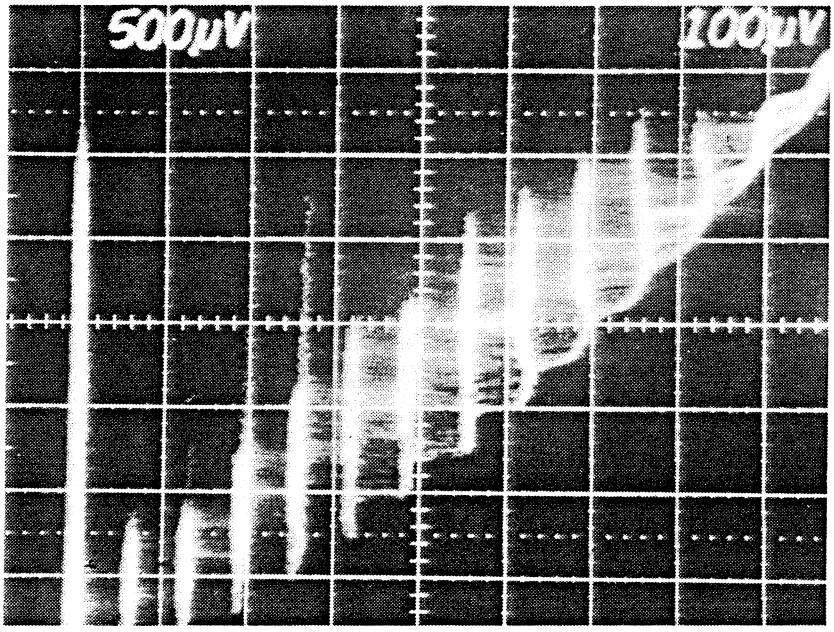

Figure 6.

(a)

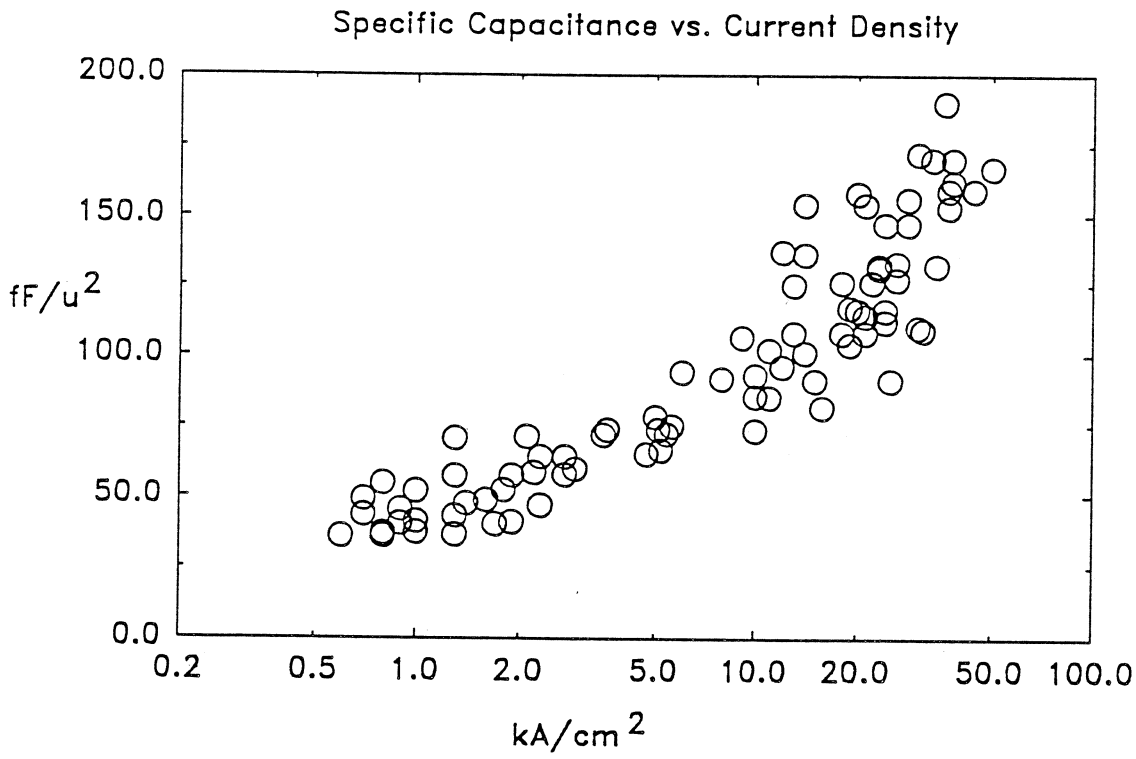
Specific Capacitance vs. Current Density
200.0
150.0
100.0
50.0
0.0
fF/u2
0.2
0.5
1.0
2.0
5.0
10.0
20.0
50.0
100.0
kA/cm 2

(b)

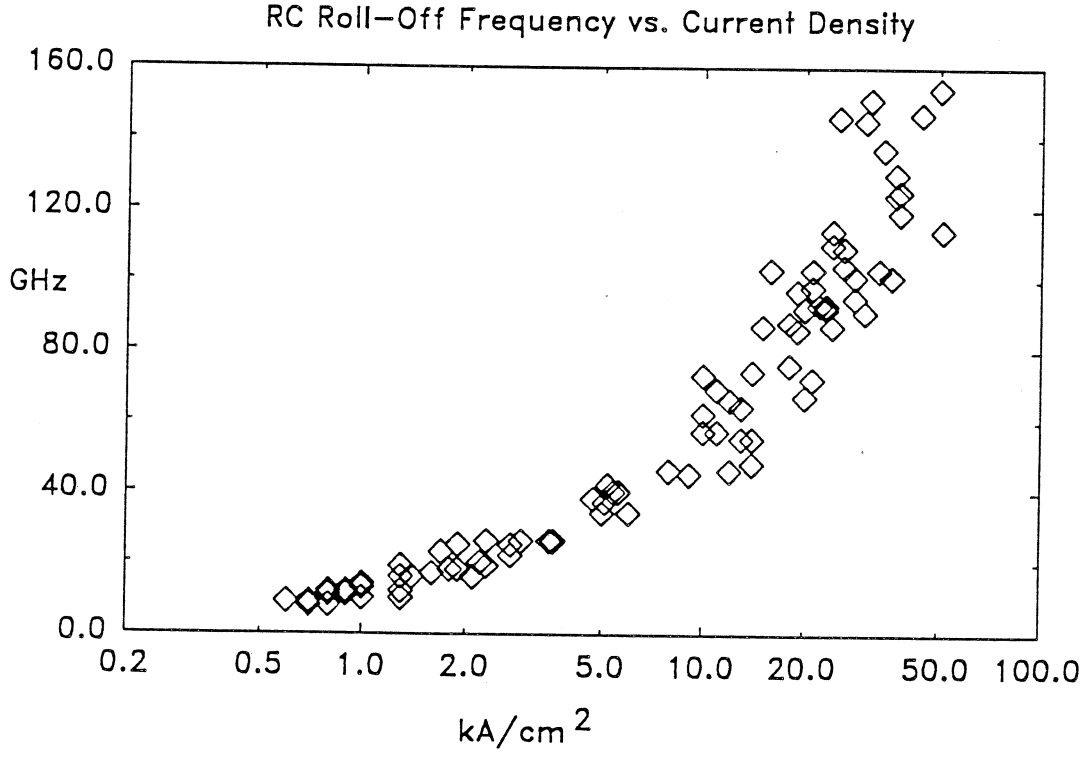
RC Roll-Off Frequency vs. Current Density
160.0
120.0
80.0
40.0
0.0
GHz
0.2
0.5
1.0
2.0
5.0
10.0
20.0
50.0
100.0
kA/cm 2